

Design Considerations and Performance of a PM Linear Actuator in a Radiation Environment

M. T. N. Mohammad*, C.N. Booth*, P. Hodgson*, L. Howlett*, P.J. Smith*, S. M. Sharkh†

*University of Sheffield, UK, m.mohammad@sheffield.ac.uk

†University of Southampton, UK, suleiman@soton.ac.uk

Keywords: PM linear actuator, Radiation Environment.

Abstract

This paper discusses design considerations for a water cooled high acceleration 3-phase air-cored brushless DC PM linear actuator used in a vacuum radiation environment. Radiation can cause damage to magnets, and the requirement for a vacuum chamber around the moving parts imposes additional constraints that further complicate the electromagnetic and mechanical design of the actuator. This paper discusses the selection of suitable materials and bearings that are compatible with operation in vacuum and can cope with the required millions of actuation cycles. The selection of suitable bearings with low friction and wear is discussed and the design of a low inertia shaft is described. The factors that have an influence on the susceptibility of the magnets to radiation damage are discussed. These factors include magnet dimensions, magnet material, external magnetic field, temperature and the directions of both the magnetic flux and radiation. FLUKA simulations are presented showing the fluences of protons, neutrons, electrons and gamma radiation to which the magnets are exposed. Based on these simulations, loss of magnetisation for different magnet materials can be predicted, and used to estimate the effect of magnet radiation ageing on actuator current, and increased temperature rise. The paper also presents transient electromagnet FEA computation of the force produced by the actuator when magnets are housed in a stainless steel vacuum chamber.

1 Introduction

As part of future experiments at the Rutherford Appleton Laboratory, a small 0.5 g titanium rectangular target plate needs to be inserted quickly and positioned accurately and reliably for 2 ms into the outer low-density halo of the accelerated proton beam inside the ISIS synchrotron particle accelerator, and then retracted rapidly [1, 2]. The distance traversed per actuation is about 44 mm in each direction; acceleration is about 780 ms^{-2} (80g) and the maximum velocity is just over 5 ms^{-1} . A prototype permanent magnet (PM) actuator (Fig. 1) was designed, built and tested to establish the feasibility of using such a device for this application [2]. FEA and experimental results presented in [2] confirmed that the actuator meets the high specific force requirements of the application. However, further research

and development was needed to establish the deterioration of the performance of the actuator due to loss of magnet magnetisation caused by radiation damage, with implications for magnet material selection and water cooling system design. It is also necessary in the actual application to enclose the actuator shuttle inside a stainless steel vacuum chamber, which will experience eddy currents whose influence on actuator force production, efficiency and temperature rise must be quantified. Additionally, work was required to design a low mass shaft, and suitable long life bearings.

This paper describes the construction of the actuator, and comments on bearing and shaft design. FLUKA [3] simulations are presented showing the fluences of different particles and gamma radiation to which the magnets will be exposed. These simulations have been used to estimate the loss of magnetisation. The increase in the current needed to compensate for this loss of magnetisation together with eddy current losses in the stainless steel vacuum chamber put further strain on the winding and water cooling system. This paper also presents transient electromagnetic FEA computations of the dynamic force produce by the actuator as it moves inside the stainless steel vacuum chamber.

2 Description of the Actuator, Mechanical Design and Material Selection

Figure 1 shows a cross-section of the actuator and figure 2 shows photographs of the stator coils and translator shuttle magnets with part of the shaft. Mounted on the top of the shaft is an optical readout vane (not shown in the figures) which monitors the position of the target and accordingly used determine the timing of electronic commutation of the current through the coils.

The actuator will be part of the accelerator system which has components sensitive to any dust generated by wear of moving parts. This dust could cause breakdown in radio frequency (RF) cavities and damage to ion pumps if it is transferred around the accelerator ring. Measures must be taken to provide robust solutions to this problem. This requires dealing with the sources of the dust to minimise this risk.

The 3-pole magnet shuttle is 18 mm long. Each magnet pole is constructed from several radially magnetised wedge shaped magnet pieces glued together on a mild steel collar attached to the titanium shaft using NM25 adhesive resin which was

selected for its high operating temperature and suitability for use in vacuum.

The stator, which is 72 mm long, comprises 24 coils mounted around a stainless steel tube, which has features on its outer surface to help locate the coils. The coils are cooled by a water pipe as illustrated in Figure 1. Split copper shims are inserted between the coils to improve cooling. The stainless steel tube is welded to end flanges to provide a means of isolating the inside of the bore which can be pumped down to a vacuum.

The stator coils were mounted outside the vacuum chamber to avoid contamination of the vacuum by out-gassing of materials such as varnish on the copper, and to ensure any degradation caused by radiation does not result in material 'crumbling' into the vacuum chamber.

However, the tube thickness needs to be kept to a minimum to keep the air-gap small and minimize deterioration of the actuator performance. The linear actuator under investigation has a tube thickness of 0.3mm and an air gap of 1.3mm. Ideally, the tube should be made of non-conducting non-magnetic material such as a machinable ceramic, to eliminate eddy currents. But stainless steel was selected for its strength, and hence small thickness, and ease of fabrication and welding.

The low inertia shaft is made from titanium. Its resonance frequency is carefully selected to be away from the nominal operation frequency of the actuator where resonance will result in the shaft fluttering to the corresponding mode shape at that frequency. Structural analysis of the shaft was carried out using ANSYS software, to make sure that shaft deflections will not exceed its design limits. This included natural frequency analysis, fatigue assessment and simulating the bending modes.

The shaft is supported vertically by a pair of plain bearings, one below and one above the magnets. The upper bearing and shaft cross-section is circular with shaft diameter of 4 mm, and bearing bore diameter of 4.1 mm. In order to maintain the correct alignment of the target and readout vane while preserving the rigidity and low mass of the shaft, the lower part of the shaft has a cross-shaped section, and passes through a similar shaped aperture in the bearing with similar clearance.

The bearings have to be designed carefully to reduce shaft friction and minimise generated dust. The bearing material has also to be chosen carefully. Long-term reliability tests proved that machinable ceramic bearings (Shapal-M) suffered unacceptable amounts of wear after only 100K actuations, and generated significant amount of grey dust. Analysis of the dust indicated a mixture of ceramic and titanium. Tests show that leaded bronze is a mechanically good bearing material but the lead and tin content of the material are not approved from a radiological point of view. An alternative to a homogeneous bearing material was to use bearings coated by diamond-like carbon (DLC). This is both very hard and smooth, and has been shown to have low friction in vacuum and good wearing properties. However, the bearings have to

be made from two halves so they can be coated with a sputtered layer of DLC 3-5 microns thick. Figure 3 shows DLC coated non-magnetic stainless steel upper bearing after 1.25M actuations.

Magnetic, non-contact bearings were ruled out as initial evaluations showed that they would add too much mass to the moving shaft. It is also not clear that they would keep the shaft on axis to the required precision (better than 0.1 mm).

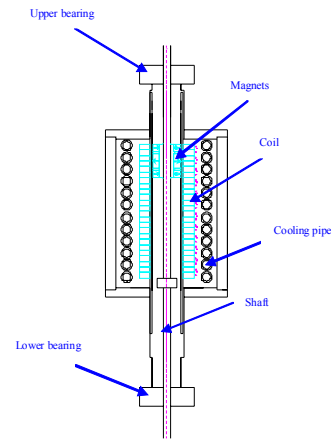


Figure 1: Cross-section of the linear actuator under investigation.



Figure 2: Photographs of the stator (left) and the PM shuttle and shaft (right).

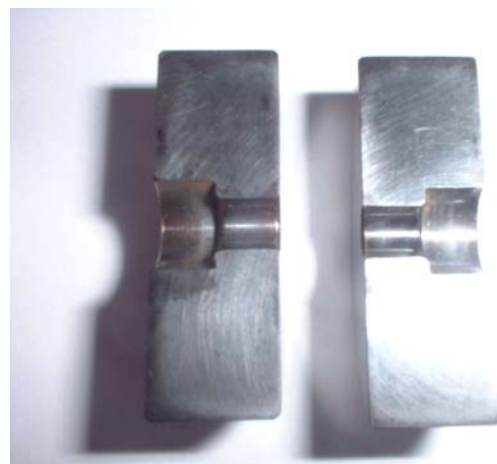


Figure 3: Non-magnetic stainless steel upper bearing after 1.25M actuations

In theory, the bearings serve only to hold the shaft on axis, where the electromagnetic forces act only axially (vertically), with no radial force component. There should therefore be no

force between bearing and shaft, and no wear should result. This is obviously not the case, as seen from the ceramic case. Preliminary studies indicated that the tolerances involved in the construction of the actuator driving the shaft should not allow significant radial forces. However, it is possible that a slight initial distortion of the shaft could lead under acceleration to flexing, significantly displacing the magnets, leading to increased off-axis forces. This can be addressed in a number of ways. More sophisticated modelling of the shaft may help to identify possible origins of the problem. Improved quality control, of bearings, magnet and coil alignment and shaft manufacture, may help to reduce forces and so bearing wear. It is important to design a stiff and stable shaft, without paying too high a price in increasing its mass.

3 Effect of Radiation on Magnets

High level radiation can cause irreversible damage to the magnets. It is believed that the mechanism by which radiation damage occurs is the transfer of energy from an incoming particle during primary collision with the magnet's atom. This raises the collision region temperature within the magnet. If this temperature rise brings the region above the Curie temperature, and the heated region is large enough, then the demagnetising field can turn the spins, and the magnetisation of a new domain occurs [4]. A number of factors are known to affect the amount of radiation damage:

A) The size, shape and orientation of the magnets (which define what we expect its internal magnetic field to be). Previous investigators have found three factors to be important. 1) The length-to-diameter ratio (L/D) of the magnet is found to have a large influence on the loss of magnetic properties when subject to radiation. Brown et al. [5] indicate that the decay rate is the greatest for the smallest L/D ratio. They also provided curves to support this for several samples having L/D ratios between 0.4 and 8.9 at different irradiation time. 2) It is also believed that the magnet size has a large influence in the amount of radiation damage. Kahkonen et al. [4], Brown et al. [5] and others reached a conclusion that larger magnets show bigger resistance to magnet damage. 3) They also found that the relationship between the direction of magnetisation and the direction of the incoming radiation has an effect. Magnets with parallel magnetisation to the incoming radiation suffer less flux loss than those magnetised in the perpendicular direction. Kahkonen explained this result in terms of the non-homogeneous magnetic field inside the magnet. The radiation damage happens more readily in regions where the magnetic field is opposite to the bulk magnetisation direction, predominantly near the surface; since the energy of the protons decreases as it passes through the magnet it is expected to do more damage closer to the proton source, and therefore the orientation of the magnet becomes important.

B) The temperature of the magnet. Magnets at higher temperature suffer more magnetisation loss. Kahkonen et al. [4] derived a formula to calculate the amount of radiation loss at different temperatures depending on the temperature and the properties of the sample.

C) The external magnetic field. Kahkonen et al. [4] present evidence that the radiation damage seems to depend linearly on the external magnetic field.

D) It is important to remember that magnets/samples from different manufacturers show differing radiation damage. Investigations show that radiation resistance increases with the amount of dysprosium (Dy) and terbium (Tb), which are added to increase coercivity. Magnets made from melt-spun ribbons show less loss of magnetisation than those of sintered magnets. Small addition of Cu, Co and O to NdFeB could reduce losses.

Publications show that Samarium Cobalt has a much higher radiation resistance than NdFeB and consequently the performance of SmCo is superior at high level of radiation. However, the superior magnetic properties of NdFeB magnets make them a good choice for many accelerator applications. For this reason there are many papers looking at their resistance to protons [4, 6, 7, 8, 9, 10], neutrons [5, 11, 12, 13, 14], electrons [15, 16, 17, 18, 19] and gammas [17, 20, 21, 22]. These studies show that the amount of demagnetisation observed is not dependent on the deposited energy, but depends on the type of particle [19]. NdFeB magnets can receive a dose of 14 MGy γ radiation without suffering any loss of magnetization, but much smaller doses of ionising radiation are capable of causing significant damage. There are many factors which influence how much radiation an NdFeB magnet can take without sustaining damage; it is therefore difficult to say what flux of a given particle type the magnets under investigations (N34KC) can sustain without suffering loss. However, the literature suggested ball park figures where less than 5 % loss in magnetisation is expected.

We have estimated the amount of radiation our magnets are exposed to, and hence made rough estimates of the consequent loss of magnetisation. Software simulation tools such as FLUKA [3], which was developed by physicists from INFN and CERN, have been used to calculate particle transport and interactions with matter. FLUKA can simulate with high accuracy the interaction and propagation inside matter of about 60 different particles, including photons, electrons and hadrons relevant in studies of the effect of material irradiation. FLUKA handles very complex geometries allowing us to simulate radiation doses and fluences from the particles created when beam particles interact with target material. Figure 4 and 5 show representative FLUKA simulation results, showing how the proton fluence decreases between target and magnets.

The data obtained from FLUKA, together with results from the literature discussed above, can be used to estimate magnet radiation damage and loss of magnetisation in our environment. Table 1 shows approximate figures for radiation that were found to cause less than 5% loss of magnetisation. The FLUKA simulation results in Table 1 put the fluences / doses of all particle types after one year of operation below the limits for 5% radiation damage, implying an adequate lifetime for the actuator. Radiation tests will be done in the near future for the N34KC and Recoma 28 magnets to confirm these results.

	Tolerable (<5% damage) values	FLUKA simulation
Protons	1 MGy	$1 \cdot 10^{13}$
Neutrons	$1 \cdot 10^{15}$	$5 \cdot 10^{14}$
Electrons	$1 \cdot 10^{15}$	$1 \cdot 10^{13}$
Gammas	14 MGy	$1 \cdot 10^{15}$
photons	-	$1 \cdot 10^{15}$

Table 1: Tolerable and expected radiation levels at the magnets after a year's running.

fluence ($\text{cm}/\text{cm}^3/\text{primary}$)

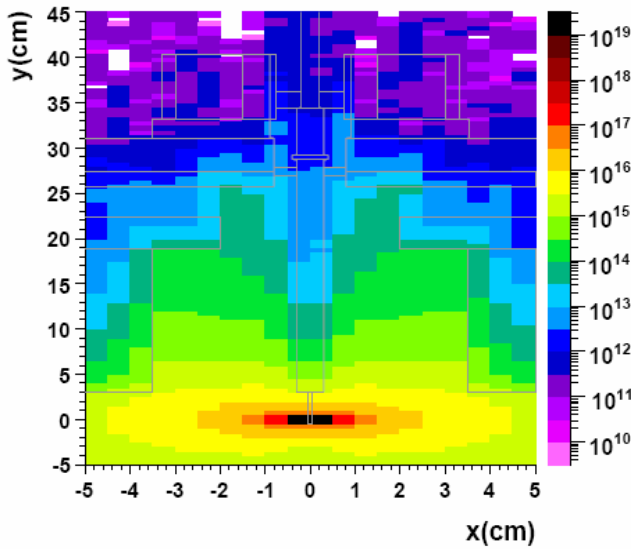


Figure 4: Proton fluence in the plane transverse to the beam. The target is at the origin, and the magnets centred at (0, 32).

fluence ($\text{cm}/\text{cm}^3/\text{primary}$)

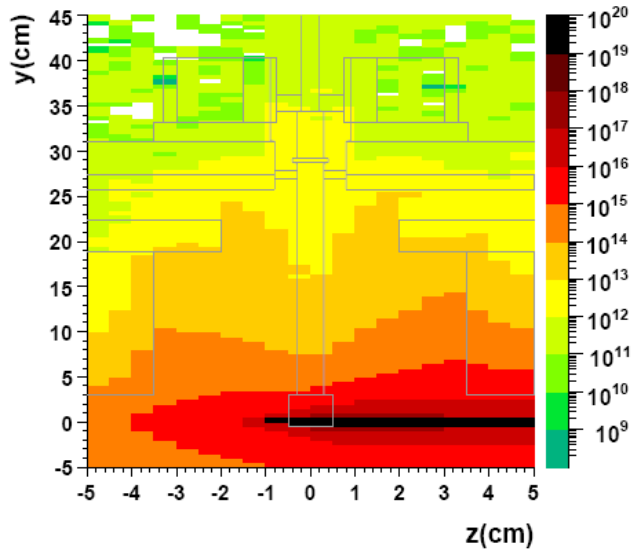


Figure 5: Proton fluence in the vertical plane containing the beam direction.

4 Electromagnetic FE Analysis

Finite element analysis was used to evaluate the electromagnetic design of the actuator. Axisymmetric models were developed using Flux-2D software of CEDRAT. No-load analysis was carried out to estimate the flux densities in magnets and coils and to calculate the back emf constant. Maximum current to operate the actuator was calculated based on the no-load results of back emf and phase shift and therefore the current motion equations were developed and used in the transient FE models.

Figure 6 shows the flux distribution when all coils are energised with a current of 37.7 A. Figure 7 shows the force capability of the design using both NdFeB ($B_r=1.2$ T) and SmCo ($B_r=1.07$ T) magnets.

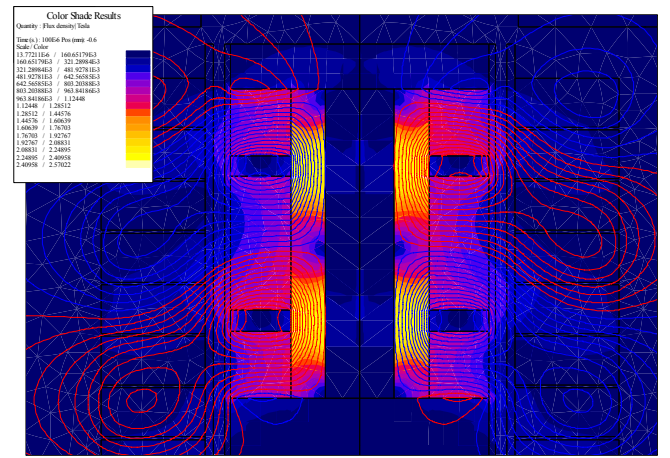


Figure 6: FE plot of flux density and lines of the actuator on load.

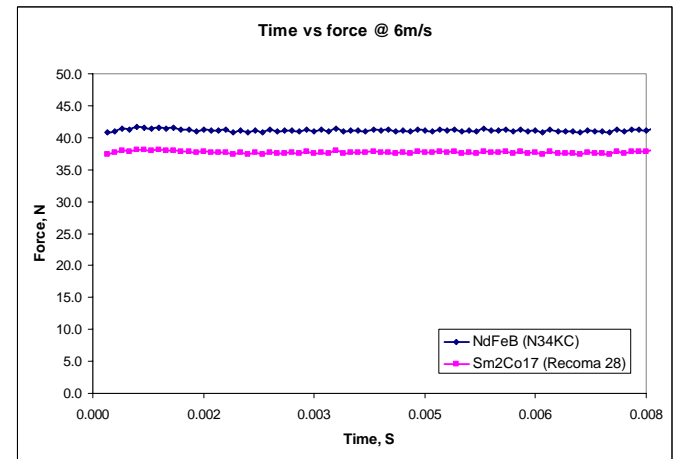


Figure 7: FE results of force capability of the linear actuator with NdFeB and SmCo magnets, $I = 37.7$ A.

The transient FE results of phase voltage and current waveforms were used to determine the requirements of the DC power supply. This includes the maximum DC link voltage of the inverter.

5 Conclusions

This paper indicates the necessity of addressing radiation issues at early design stages to obtain a sustainable electromagnetic and thermal operation of a linear actuator. It is necessary to consider a safety factor so that the design can cope with the extra temperature rise caused by applying more current in case of loss of magnetisation.

The complication, constraints and restrictions of the mechanical construction have also been investigated.

A review of the literature indicates that there are many factors which influence the susceptibility of magnets to radiation damage. These include magnet dimensions, magnet material, and external magnetic field and temperature. Simulations, however, indicate that an adequate magnet lifetime can be obtained for our application.

Acknowledgement

The authors would like to thank the Rutherford Appleton Laboratory and Science & Technology Facilities Council (STFC) for funding and supporting this work.

References

- [1] Web site: <http://www.isis.rl.ac.uk/>
- [2] Schofield, N, Smith, P.J. and Booth, C, "A low mass, brushless permanent magnet linear actuator for the ISIS target accelerator", Paper FF-12, 50th Annual Conference on Magnetism and Magnetic Materials (MMM05), San Jose, California, USA, Oct. 30 - 3 Nov. 2005.
- [3] A. Fasso et al. FLUKA: a multi-particle transport code. CERN-2005-10, INFN/TC 05/11, SLAC-R-773, 2005.
- [4] Kahkonen et al. Radiation damage in Nd-Fe-B magnets: temperature and shape effects. *J. Phys. Condensed Matter*, 4:1002-1014, 1992.
- [5] R.D. Brown and J.R. Cost. Radiation-induced changes in magnetic properties of Nd-Fe-B permanent magnets. *IEEE Trans. Mag.*, 25:3117-3120, 1989.
- [6] Talvitie et al. Magnetic flux loss in Nd-Fe-B magnets irradiated with 20 MeV protons. *J. Mag. Mat.*, 102:323-330, 1991.
- [7] E.W. Blackmore. Radiation effects of protons on samarium-cobalt permanent magnets. *IEEE, NS-32* 5:3669-3671, 1985.
- [8] F. Coninckx. Radiation effects on rare-earth cobalt permanent magnets. CERN/SPS 83-1.
- [9] Kahkonen et al. Effects of proton and α irradiation on permanent magnets. *Phys. Rev. B*, 49:6052-6057, 1994.
- [10] Kahkonen et al. Effect of high temperature irradiation on SmCo permanent magnets. *J. Appl. Phys.*, 72:2075-2076, 1992.
- [11] J. Allen et al. Radiation damage studies with hadrons on materials and electronics. Presented at the 9th European Particle Accelerator Conference (EPAC 2004), Lucerne, Switzerland, 5-9 Jul 2004
- [12] R.D. Brown et al. Neutron irradiation study on Nd-Fe-B permanent magnets made from melt spun ribbons. *J. Appl. Phys.*, 64:5305-5307, 1988.
- [13] J.R. Cost et al. Effects of neutron irradiation on Nd-Fe-B magnetic properties. *IEEE Trans. Mag.*, 24:2016-2019, 1988.
- [14] X.M. Marechal et al. 65 MeV neutron irradiation of Nd-Fe-B permanent magnets. Presented at the 10th European Particle Accelerator Conference (EPAC 06), Edinburgh, Scotland, 26-30 Jun 2006.
- [15] T. Bizen et al. Demagnetization of undulator magnets irradiated by high energy electrons. *NIM A*, 467-468:185-189, 2001.
- [16] T. Bizen et al. Baking effects for NdFeB magnets against demagnetization induced by high-energy electrons. *NIM A*, 515:850-852, 2003.
- [17] T. Ikeda and S. Okuda. Magnetic flux loss of the permanent magnets used for the wigglers of FELs by the irradiation with high-energy electrons or x-rays. *NIM A*, 407:439-442, 1998.
- [18] N. Kobayashi, S. Okuda, K. Ohashi. Effects of electron-beam and γ -ray irradiation on the magnetic flux of Nd-Fe-B and Sm-Co permanent magnets. *NIM B*, 94:227-230, 1994.
- [19] J. Pfulger et al. Radiation exposure and magnetic performance of the undulator system for the VUV FEL at the TESLA test facility phase-1 after 3 years of operation. *NIM A*, 507:186-190, 2003.
- [20] P. Van Vaerenbergh et al. Ageing of permanent magnet devices at the ESRF. Fifth European Conference on Radiation and its Effects. RADECS 99. 1999
- [21] I. Vasserman J. Pfluger, G. Heintz. Search for possible radiation damage on a NdFeB permanent magnet structure after two years of operation. *Rev. Sci. Instrum.*, 66:1946-1948, 1995.
- [22] K. Boockmann et al. Effect of γ -radiation on Sm-Co and Nd-Dy-Fe-B-magnets. *J. Mag. Mat.*, 101:345-346, 1991.